

Title No. 119-S29

# Simplified Strut-and-Tie Model for Shear Strength Prediction of Reinforced Concrete Low-Rise Walls

by Jimmy Chandra and Susanto Teng

*In this study, an analytical model using the strut-and-tie concept was developed to predict reinforced concrete (RC) low-rise wall shear strengths. In the model, the failure mode considered was crushing of the diagonal compression strut. To accurately determine the strut area, a formula for calculating depth of compression zone at the bottom of wall was derived with the aid of nonlinear finite element analysis. A total of 100 RC low-rise wall specimens failing in shear obtained from available literature were used to verify the accuracy of wall strength predictions of the proposed strut-and-tie model. Furthermore, strength predictions from building codes and other analytical models were also included for comparison purposes. The analysis results show that the proposed strut-and-tie model is conservative and it has the lowest coefficient of variation as compared to other methods in predicting the shear strength of RC low-rise walls. In addition, the predictions of the proposed model are quite consistent and less scattered for wide ranges of wall height-length ratios and concrete compressive strengths.*

**Keywords:** building code predictions; reinforced concrete (RC) wall shear strengths; strut-and-tie.

## INTRODUCTION

The use of reinforced concrete (RC) walls has become increasingly popular nowadays due to their superior performance against lateral loads such as wind and earthquake loads.<sup>1</sup> In addition, not only for lateral loads, RC walls can also be used to resist gravity loads as well. Thus, it is important to be able to determine the strength of RC walls accurately to provide safe and economical design, as these are two major concerns for structural engineers. Previous studies by the authors<sup>2,3</sup> show that the flexural strength of RC walls can be reasonably well predicted using flexural theory for members subjected to axial load and bending moment. However, for the shear strength, empirical building code formulas<sup>4,5</sup> underestimate RC wall shear strengths by a significant margin, especially for high-strength concrete (HSC) walls, and the overall predictions are quite scattered. Therefore, there was a need to develop an analytical model based on rational theory to accurately predict the shear strength of RC walls.

The rational theory for predicting RC members' shear strength was developed in early 1900s based on the truss analogy.<sup>6,7</sup> The theory was further developed to predict the shear strength of RC members more accurately.<sup>8,9</sup> For RC low-rise walls having a height-length ratio ( $H_w/L_w$ ) less than 2.5, many researches have been conducted to predict the shear strength.<sup>10-13</sup> All those theories are able to predict the shear strength of RC low-rise walls with certain accuracy. However, in their truss models, it was assumed that

shear stress distribution over an entire wall cross section was uniform which is only valid for RC low-rise walls with boundary elements having  $H_w/L_w$  less than 1.0.<sup>10,11</sup> Moreover, the calculation of RC low-rise wall shear strengths using their models needs an iterative procedure to obtain a solution that satisfies equilibrium and compatibility conditions as well as constitutive law of materials. Thus, it may not be practical to be used by engineers to estimate the shear strength of RC low-rise walls.

In this study, an analytical model for predicting RC low-rise wall shear strengths was developed based on the strut-and-tie concept. RC low-rise walls having  $H_w/L_w$  less than 2.5 can be categorized as disturbed regions where a plane section does not remain plane. In this case, the strut-and-tie model is considered as a rational approach to predict the strength of disturbed regions.<sup>14</sup> Later on, experimental wall strengths obtained from available literatures were used to verify the accuracy of the proposed strut-and-tie model. In addition, strength predictions from building codes<sup>4,5</sup> and other strut-and-tie models<sup>15,16</sup> were included as well for comparison purposes.

## RESEARCH SIGNIFICANCE

This study focused on the development of an analytical model based on the strut-and-tie concept to predict RC low-rise wall shear strengths. It is expected that the model could serve as a rational yet simple approach for predicting the shear strength of RC low-rise walls. Furthermore, the study conducted here provides a new formula for calculating the depth of the compression zone at the bottom of RC low-rise walls in which the assumption of plane section remains plane (linear strain distribution) is not valid. The formula was developed with the aid of nonlinear finite element analysis (FEA) using ATENA software.<sup>17</sup> This is important to accurately predict the shear strength of RC low-rise walls.

## BUILDING CODES AND OTHER ANALYTICAL MODELS

ACI 318-19<sup>4</sup> and Eurocode 8<sup>5</sup> are two reference building codes that are adopted in many countries. As such, those two

*ACI Structural Journal*, V. 119, No. 2, March 2022.

MS No. S-2020-477.R1, doi: 10.14359/51734330, received July 3, 2021, and reviewed under Institute publication policies. Copyright © 2022, American Concrete Institute. All rights reserved, including the making of copies unless permission is obtained from the copyright proprietors. Pertinent discussion including author's closure, if any, will be published ten months from this journal's date if the discussion is received within four months of the paper's print publication.

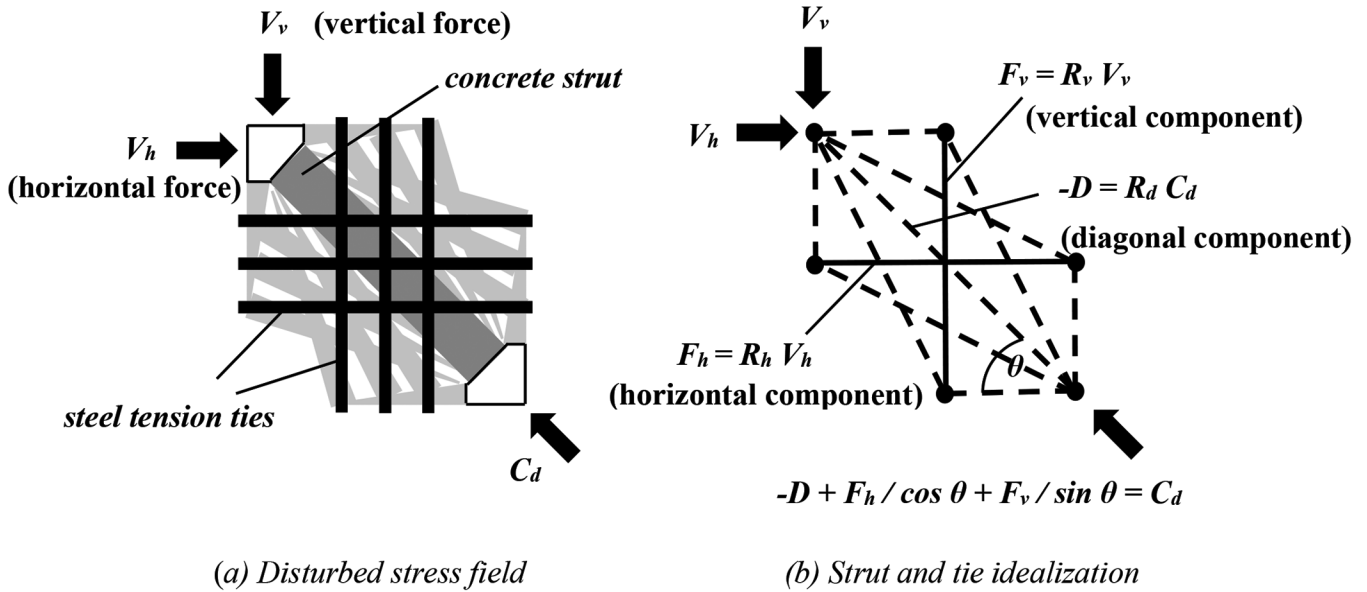


Fig. 1—Strut-and-tie mechanisms proposed by Hwang and Lee.<sup>15</sup>

building codes and other strut-and-tie models proposed by other researchers<sup>15,16</sup> are reviewed briefly as follows.

#### ACI 318-19

According to ACI 318-19,<sup>4</sup> the nominal shear strength  $V_n$  of RC special structural walls can be calculated as follows

$$V_n = A_{cv} (\alpha_c \lambda \sqrt{f'_c} + \rho_t f_{yt})$$

ACI 318-19 also states that the value of  $V_n$  shall not exceed  $0.83A_{cv}\sqrt{f'_c}$  (in N).

#### Eurocode 8 (EN 1998-1:2004)

According to Eurocode 8<sup>5</sup> (EC8), the shear strength of RC walls subjected to earthquake loadings can be taken as the lesser value of shear resistance from two failure modes: 1) diagonal compression failure  $V_{Rd,max}$ ; and 2) diagonal tension failures, either  $V_{Rd,s}$  or  $V_{Rd}$ .

*Diagonal compression failure of web due to shear*—For the case of diagonal compression failure, the shear strength is calculated as follows

$$V_{Rd,max} = \alpha_{cw} b_w z v_1 f_{cd} / (\cot \theta + \tan \theta) \quad (1)$$

where the recommended value of  $\alpha_{cw}$  is as follows

$$1.0 \text{ for non-prestressed structures} \quad (1a)$$

$$(1.0 + \sigma_{cp}/f_{cd}) \text{ for } 0 < \sigma_{cp} \leq 0.25f_{cd} \quad (1b)$$

$$1.25 \text{ for } 0.25f_{cd} < \sigma_{cp} \leq 0.5f_{cd} \quad (1c)$$

$$2.5 (1.0 - \sigma_{cp}/f_{cd}) \text{ for } 0.5f_{cd} < \sigma_{cp} < 1.0f_{cd} \quad (1d)$$

The recommended value for  $v_1$  is  $0.6 [1.0 - f_{ck}/250]$  ( $f_{ck}$  in MPa).

EC8 recommends that the values of  $\cot \theta$  and  $\tan \theta$  are taken as 1.0.

*Diagonal tension failure of web due to shear*—If  $\alpha_s = M_{Ed}/(V_{Ed}L_w) \geq 2.0$ , where  $M_{Ed}$  is the design bending moment at the base of the wall and  $V_{Ed}$  is the design shear force, the shear strength is given by  $V_{Rd,s}$

$$V_{Rd,s} = \frac{A_{sw}}{s} z f_{ywd} \cot \theta \quad (2)$$

If  $\alpha_s = M_{Ed}/(V_{Ed}L_w) < 2.0$ , the shear strength is given by  $V_{Rd}$

$$V_{Rd} = V_{Rd,c} + 0.75 \rho_h f_{yd,h} b_{wo} \alpha_s L_w \quad (3)$$

#### Hwang and Lee's model

Hwang and Lee<sup>15</sup> proposed a softened strut-and-tie model for calculating the shear strength of RC walls. The model has the term “softened” because it takes into account the softening behavior of cracked concrete. In the model, the external forces were resisted by a combination of concrete compression struts and steel tension ties as shown in Fig. 1. There are three load paths—that is, vertical, horizontal, and diagonal components which are calculated according to their relative stiffness ( $R_v$ ,  $R_h$ , and  $R_d$ ), and these components are combined together to become the diagonal compression force acting on nodal zone  $C_d$ . The nominal capacity of the nodal zone can be calculated using Eq. (4a). Then, the shear strength of RC wall according to this model can be taken as the horizontal component of the diagonal compression force that is corresponding to the nominal capacity of the nodal zone

$$C_{d,n} = K \zeta f'_c A_{str} \quad (4a)$$

where  $K$  is strut-and-tie index, which is defined as follows

$$K = \frac{-D + \frac{F_h}{\cos \theta} + \frac{F_v}{\sin \theta}}{-D + \frac{F_h}{\cos \theta} \left(1 - \frac{\sin^2 \theta}{2}\right) + \frac{F_v}{\sin \theta} \left(1 - \frac{\cos^2 \theta}{2}\right)} \geq 1.00 \quad (4b)$$

and  $\zeta$  is softening coefficient of cracked diagonal concrete strut, which in this model, it is calculated as  $(3.35/\sqrt{f'_c}) \leq 0.52$ .

### Kassem's model

Kassem<sup>16</sup> proposed a strut-and-tie model and closed-form design formula for predicting the shear strength of squat walls. The model uses three shear-resisting mechanisms—that is, diagonal, horizontal, and vertical mechanisms—similar to Hwang-Lee's model.<sup>15</sup> In this model, a parametric expression to calculate the shear strength of squat walls was developed and calibrated using data of 645 walls obtained from literature. The design formulas developed are as follows (in SI units):

For walls with rectangular cross section

$$V_n = 0.27 f'_c \left[ \psi k_s \sin(2\theta) + 0.11 \omega_h \frac{H'}{d_w} + 0.30 \omega_v \cot(\theta) \right] t_w d_w \leq 0.83 \sqrt{f'_c} t_w d_w \quad (5a)$$

For walls with flanged cross section

$$V_n = 0.47 f'_c \left[ \psi k_s \sin(2\theta) + 0.15 \omega_h \frac{H'}{d_w} + 1.76 \omega_v \cot(\theta) \right] t_w d_w \leq 1.25 \sqrt{f'_c} t_w d_w \quad (5b)$$

### PROPOSED STRUT-AND-TIE MODEL

In this study, an analytical model for predicting RC low-rise wall shear strengths was developed based on the strut-and-tie concept. The behavior of RC low-rise wall having a height-length ratio ( $H_w/L_w$ ) less than 2.5 is dominated by shear mode<sup>18,19</sup> and it can be categorized as a disturbed region where a plane section does not remain plane and shear stress is not uniform within the wall panel. Thus, the strut-and-tie model is considered a more appropriate approach to predict the strength as compared to the sectional design model which includes concrete resistance to shear  $V_c$  due to tensile stresses in concrete.<sup>14,20</sup> In contrast to Hwang and Lee's softened strut-and-tie model<sup>15</sup> that uses three compression struts, the model developed in this study uses only one diagonal compression strut to be simple. Furthermore, the contribution of web reinforcement is accounted in terms of confinement effect to the diagonal compression strut.

### Equilibrium of proposed strut-and-tie model

Initially, a typical RC low-rise wall with axial load  $P$  and lateral load  $V$  as displayed in Fig. 2 has reaction forces at the bottom of the wall—that is, horizontal reaction force that is equal to  $V$ , vertical reaction force, and bending moment that can be represented by a combination of tension force  $T$  and compression force  $C$ . To simplify the load transfer

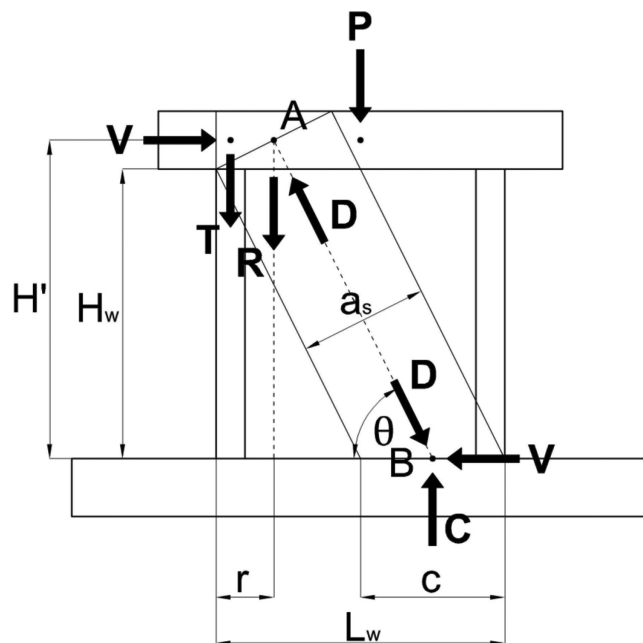


Fig. 2—Equilibrium of proposed strut-and-tie model.

mechanism, a resultant force  $R$  is used to replace the axial load  $P$  and tension force  $T$  in the equilibrium equation. The resultant force  $R$  and lateral load  $V$  are equilibrated at point  $A$  by diagonal compression force  $D$  and thus, it forms a strut-and-tie model. The diagonal compression force  $D$  is equilibrated at point  $B$  by compression force  $C$  and horizontal reaction force that is equal to  $V$ . The governing failure mode of the model is crushing of diagonal compression strut which represents shear failure of the wall web. The internal and external forces equilibrium of the model is described as follows

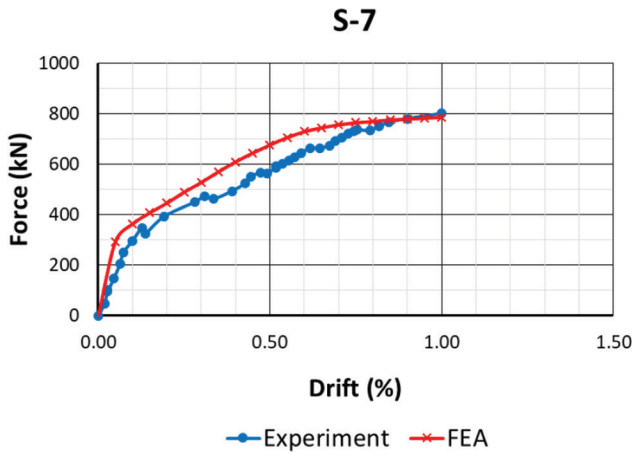
$$R = C = D \sin \theta \quad (6)$$

$$V = D \cos \theta \quad (7)$$

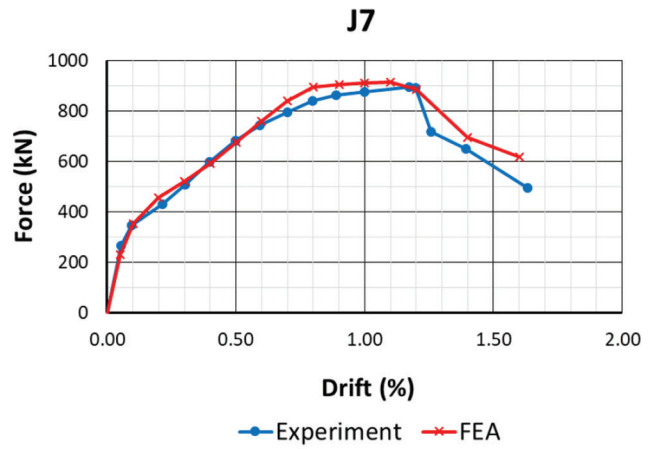
### Determination of depth of compression zone at bottom of wall

In this model, depth of compression zone at the bottom of wall  $c$  as displayed in Fig. 2 has to be determined first before calculating the diagonal compression strut capacity. Initially, the authors calculated the depth of compression zone  $c$  based on flexural theory with the assumption of linear strain distribution along the wall cross section. Nevertheless, this assumption led to inaccurate predictions of RC wall shear strengths. This was because the assumption might not be valid for RC low-rise wall that can be categorized as disturbed region in which a plane section does not remain plane. Thus, in this model, the value of  $c$  is calculated using a formula that was derived using nonlinear FEA.

First, some parameters that influence the depth of the compression zone were identified. Based on flexural theory, these parameters are concrete strength  $f'_c$ , vertical reinforcement area in the edge column or boundary element  $A_{sb}$ , and value of axial load  $P$ . Referring from the flexural theory for a member subjected to axial load and bending moment, it is



(a)



(b)

Fig. 3—Comparison of envelope curves between experimental result and finite element analysis (FEA): (a) Specimen S-7 tested by Gupta and Rangan<sup>12</sup>; and (b) Specimen J7 tested by Teng and Chandra.<sup>22</sup> (Note: 1 kN = 0.22 kip.)

clear that the value of  $c$  decreases if the value of  $f'_c$  increases. In contrast, the value of  $c$  increases if the value of  $A_{sb}$  or  $P$  increases. Moreover, the authors added shear span ratio or wall height-length ratio ( $H_w/L_w$ ) as additional parameter that affects the value of  $c$ . This was because in similar cases of disturbed region—that is, deep beams—it was shown that the value of  $c$  increases if the shear span ratio decreases.<sup>21</sup>

Second, after identifying parameters influencing the value of  $c$  and their qualitative relationships, the following step was to determine quantitative relationships between these parameters and the value of  $c$ . The main objective was to express the value of  $c$  as a function of these parameters ( $f'_c$ ,  $A_{sb}$ ,  $P$ , and  $H_w/L_w$ ). For this objective, nonlinear FEA using ATENA software<sup>17</sup> was used to determine multiplication factors for each parameter. The software was used because its superior capability to perform nonlinear analysis of RC structures and it has advanced material models for concrete and steel reinforcement. In this study, RC wall specimen S-7 having  $H_w/L_w$  of 1.0 tested by Gupta and Rangan<sup>12</sup> and RC wall specimen J7 having  $H_w/L_w$  of 2.0 tested by Teng and Chandra<sup>22</sup> were used to validate the accuracy of the finite element model. The comparison of envelope curves between experimental result and FEA of those specimens is displayed in Fig. 3. It can be seen that the finite element model can predict well the force-drift relationship of those specimens.

Subsequently, a parametric study using a typical wall specimen similar to the ones tested by Teng and Chandra<sup>22</sup> with varying parameters mentioned earlier was done to obtain the value of  $c$  at the peak loading condition of each specimen. For concrete strength, two values were used—that is,  $f'_c = 50$  and 100 MPa (7.25 and 14.50 ksi). For vertical reinforcement area in the edge column or boundary element, two values were used—that is,  $A_{sb} = 1200$  and 2400 mm<sup>2</sup> (1.86 and 3.72 in.<sup>2</sup>). For axial force, three values of axial load ratio (ALR) were used—that is, 0.0, 0.1, and 0.2. For  $H_w/L_w$ , three values were used—that is, 0.4, 1.0, and 2.0. In addition, the authors also attempted to vary the boundary element width  $b_f$ —that is, 120, 250, and 500 mm (4.72, 9.84, and 19.69 in.)—to observe the relationship between  $c$  and  $b_f$ .

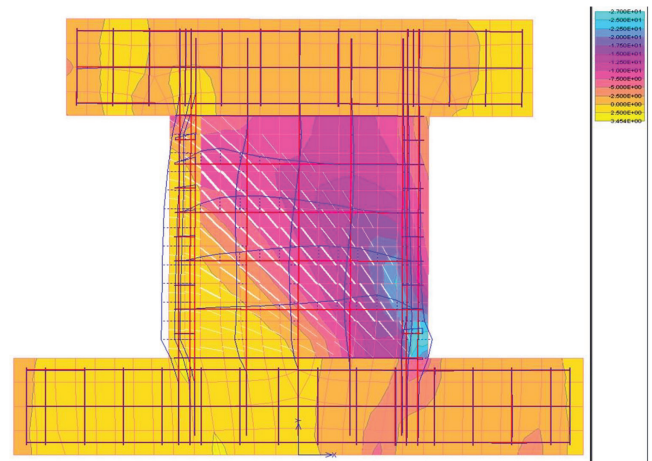


Fig. 4—State of normal stresses in vertical axis at maximum lateral load of typical wall specimen analyzed using ATENA software.<sup>17</sup>

An example of analysis results of a typical wall specimen is displayed in Fig. 4.

In total, 108 specimens were analyzed and the values of  $c$  obtained at the peak loading condition of each specimen were measured. These values were then plotted against varying parameters to obtain the quantitative relationships. These relationships can be seen in Fig. 5 to 7. The parameters  $f'_c$  and  $P$  are combined into one and normalized with wall web area to become  $P/(f'_c A_w)$  because this is more frequently used as a parameter. From the figures, it can be seen that the value of  $c$  increases linearly with increment of  $P/(f'_c A_w)$  and  $A_{sb}/A_w$ . In contrast, the value of  $c$  decreases exponentially with increment of  $H_w/L_w$ . These analysis results are consistent with qualitative relationships mentioned previously. Hence, the value of  $c$  can be expressed as follows

$$c = L_w \left( c_1 + c_2 \frac{P}{f'_c A_w} + c_3 \frac{A_{sb}}{A_w} \right) \left( \frac{H_w}{L_w} \right)^{c_4} \leq d_w \quad (8)$$

Equation (8) contains four constants that need to be determined. Constants  $c_2$ ,  $c_3$ , and  $c_4$  can be derived from Fig.

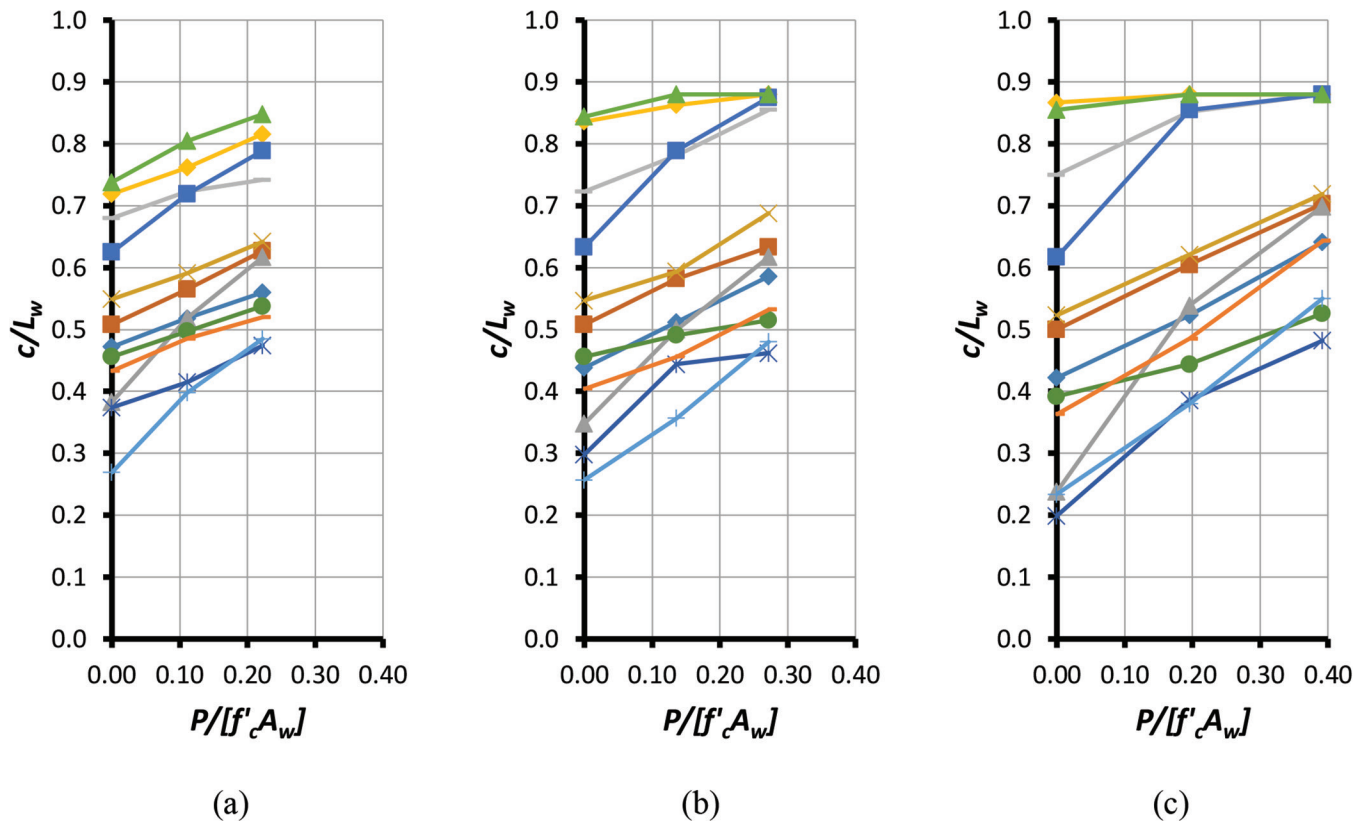


Fig. 5—Values of  $c/L_w$  obtained from nonlinear FEA plotted against  $P/[f'_c A_w]$ : (a) cases for  $b_f = 120$  mm (4.72 in.); (b) cases for  $b_f = 250$  mm (9.84 in.); and (c) cases for  $b_f = 500$  mm (19.69 in.).

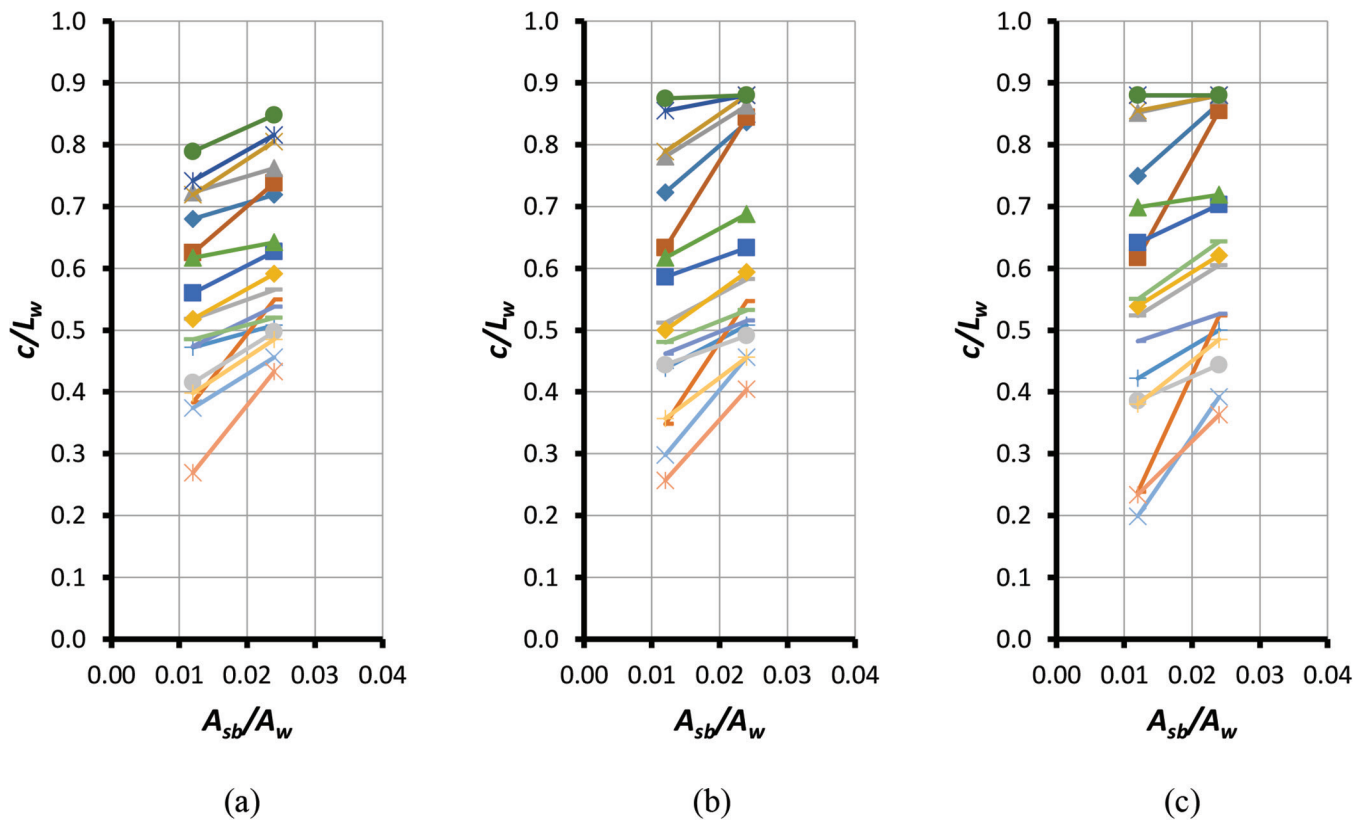


Fig. 6—Values of  $c/L_w$  obtained from nonlinear FEA plotted against  $A_{sb}/A_w$ : (a) cases for  $b_f = 120$  mm (4.72 in.); (b) cases for  $b_f = 250$  mm (9.84 in.); and (c) cases for  $b_f = 500$  mm (19.69 in.).

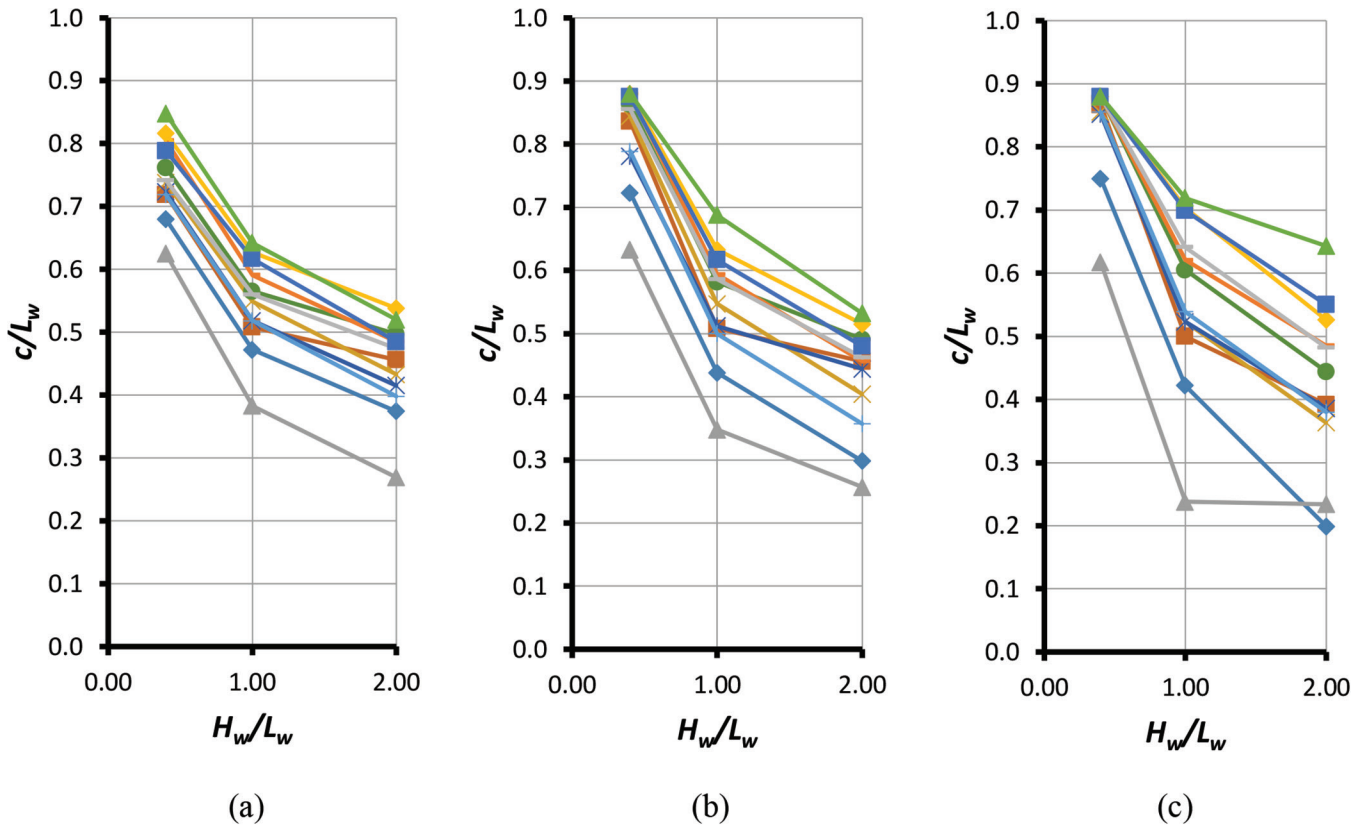


Fig. 7—Values of  $c/L_w$  obtained from nonlinear FEA plotted against  $H_w/L_w$ : (a) cases for  $b_f = 120$  mm (4.72 in.); (b) cases for  $b_f = 250$  mm (9.84 in.); and (c) cases for  $b_f = 500$  mm (19.69 in.).

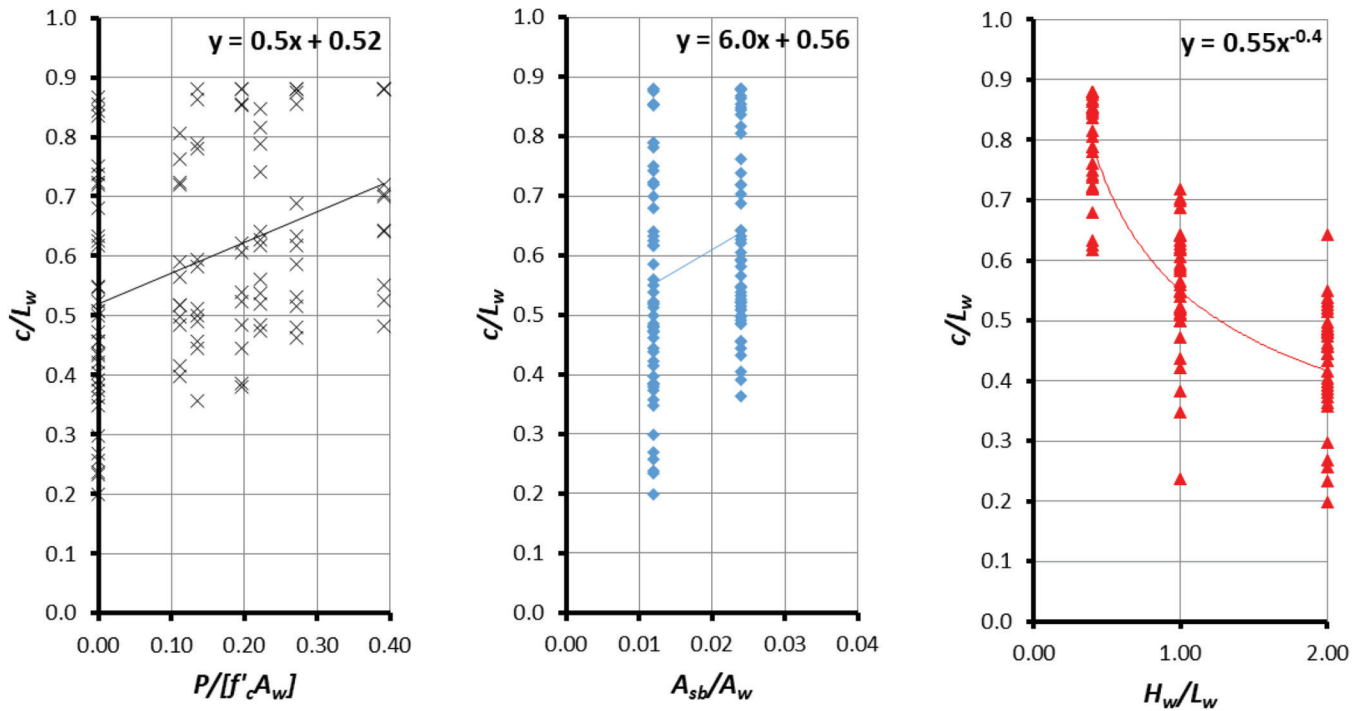


Fig. 8—Relationships between  $c$  and varying parameters with average regression lines and their equations.

5 to 7 by plotting regression lines for each data series. From the equations of the regression lines, the constants were obtained and then the average constant value from all data series was calculated. The average regression lines as well as the average constant values are presented in Fig. 8. From

the figure, the values of  $c_2$ ,  $c_3$ , and  $c_4$  were determined as 0.5, 6.0, and  $-0.4$ , respectively. Subsequently, the value of  $c_1$  was obtained by trial-and-error approach to achieve the most suitable values of  $c$  that were in good agreement with the values of  $c$  obtained from nonlinear FEA. Thus, the value of

$c_1$  was found to be 0.35. Moreover, from the nonlinear FEA, it was noted that the value of  $c$  should not be taken greater than effective depth of wall  $d_w$ . In this model,  $d_w$  is defined as the distance from center to center of the edge columns or boundary elements or it can be taken as 80% of wall length  $0.8L_w$  in the case of an RC wall without edge columns or boundary elements.

### Capacity of diagonal compression strut

Capacity of the diagonal compression strut  $D_n$  is a product of effective strut strength  $\zeta f'_c$  and the strut area  $A_{str}$  as described by

$$D_n = \zeta f'_c A_{str} \quad (9)$$

In this model, the value of effective strut strength is taken as recommended by Eurocode 2.<sup>23</sup> The code considers reduction of concrete strut strength due to tensile stresses that cause cracks in the concrete strut. Moreover, in this model, increment of concrete strut strength because of confinement effect from transverse reinforcement is also considered using recommendation by FIP Commission 3.<sup>24</sup> Thus, the softening coefficient for strut strength  $\zeta$  in this model can be described as follows

$$\zeta = 0.6 (1 - f'_c/250) \times 0.80 (1 + 1.6\alpha_w\omega_w) \leq 0.85 \quad (10)$$

where  $\alpha_w$  and  $\omega_w$  are defined as

$$\alpha_w = 1.6 \frac{s}{t_w} \leq 0.4 \quad (11)$$

$$\omega_w = 4 \frac{\rho f_y}{f'_c} \quad (12)$$

Because the definition of transverse reinforcement herein that provides confinement effect to the concrete strut is the one that is perpendicular to the strut axis, it is needed to represent vertical and horizontal web reinforcement of the RC low-rise wall to be the transverse reinforcement of the concrete strut as defined by FIP Commission 3.<sup>24</sup> Therefore, in this model, the term  $\rho f_y$  is represented as

$$\rho f_y = \rho_v f_{yv} \cos \theta + \rho_h f_{yh} \sin \theta \quad (13)$$

where  $\theta$  is defined as

$$\theta = \tan^{-1} \left( \frac{H'}{L_w - r - 0.5c} \right) \quad (14)$$

In this model, the value of  $\theta$  is limited to  $31 \leq \theta \leq 59$  degrees.

The strut area  $A_{str}$  is defined as a product of strut depth multiplied by strut width. Strut depth  $a_s$  is the perpendicular projection of depth of compression zone at the bottom of wall  $c$  to the strut axis as displayed in Fig. 2, while strut width can simply be taken as the thickness of wall web  $t_w$ . Finally, the nominal wall shear strength due to crushing of diagonal compression strut  $V_n$  is defined as

$$V_n = D_n \cos \theta \quad (15)$$

An example of RC wall shear strength calculation using the proposed strut-and-tie model can be seen in the Appendix.

### COMPARISON WITH EXPERIMENTAL RESULTS

To examine the accuracy of the proposed strut-and-tie model, experimental wall strengths of 100 specimens collected from past experiments on RC low-rise walls failing in shear<sup>12,19,22,25-37</sup> were compared with calculated shear strengths from the model. Subsequently, the predictions from the proposed strut-and-tie model were also compared with predictions from building codes<sup>4,5</sup> and other strut-and-tie models.<sup>15,16</sup> The analysis results are presented in terms of ratio of the experimental shear strengths to calculated shear strengths  $V_{exp}/V_n$ . The ratio below 1.00 means that the prediction overestimates the shear strength whereas the ratio above 1.00 means that the prediction underestimates the shear strength. These results are presented in Table 1. Moreover, the ratio was also plotted against  $H_w/L_w$  (refer to Fig. 9) and  $f'_c$  (refer to Fig. 10) to observe the variation of predictions as affected by those parameters.

From the statistical parameters of  $V_{exp}/V_n$  as presented in Table 1, it can be concluded that on average, all methods are conservative in predicting the shear strength of RC low-rise walls. Hwang and Lee's model<sup>15</sup> has the average value  $V_{exp}/V_n$  of 1.29, which is the closest to 1.00 but overestimates the shear strength of many RC low-rise walls (approximately 22 out of 100 specimens), whereas the proposed strut-and-tie model only overestimates seven out of 100 specimens. This means Hwang and Lee's model<sup>15</sup> needs a lower strength reduction factor (below 0.68) as compared to the proposed model (approximately 0.83) to ensure safe predictions of RC low-rise wall shear strengths. The proposed model has the average value  $V_{exp}/V_n$  of 1.35, which is the second closest to 1.00 and it has the lowest coefficient of variation (COV) of 0.19 as compared to other methods. This is definitely an advantage of the proposed model over other methods. Furthermore, as can be seen in Table 1, Eurocode 8<sup>5</sup> is indeed the most conservative method with average value  $V_{exp}/V_n$  of 2.13 and the code underestimates the shear strength of all 100 specimens collected in this study. Moreover, Kassem's model<sup>16</sup> has the highest COV of 0.37 with the average value  $V_{exp}/V_n$  of 1.40 while ACI 318<sup>4</sup> has similar average value  $V_{exp}/V_n$  (1.41) and slightly lower COV (0.35).

From Fig. 9 and 10, it can be seen that the predictions of the proposed strut-and-tie model are quite consistent and less scattered for various ranges of  $H_w/L_w$  and  $f'_c$ , as compared to the predictions by other methods. From Fig. 9, it can be seen that ACI 318-19<sup>4</sup> is more conservative for walls with lower  $H_w/L_w$  while it is the opposite for Hwang and Lee's model<sup>15</sup> and Kassem's model.<sup>16</sup> From Fig. 10, except for Kassem's model,<sup>16</sup> it can be seen that the predictions of most methods are closer to 1.00 for walls with  $f'_c$  below 60 MPa (8.70 ksi) and they are more conservative for walls with  $f'_c$  above 60 MPa (8.70 ksi). In addition, the predictions of Eurocode 8<sup>5</sup> are quite scattered for various ranges of  $H_w/L_w$  and  $f'_c$ , and there is no clear trend that can be observed from these figures.

**Table 1—Ratio of experimental and calculated wall shear strengths**

No.	Specimen ID	$f_c'$ , MPa	$P/(f_c'A_g)$	$H_w/L_w$	$\rho_{vf}$ , MPa	$\rho_{vfy}$ , MPa	$V_{exp}/V_n$				
							ACI 318-19 <sup>4</sup>	EC8 <sup>5</sup>	Hwang-Lee <sup>15</sup>	Kassem <sup>16</sup>	Proposed model
Hirosawa <sup>25</sup>											
1	72	17	0.12	0.94	2.07	1.09	1.33	1.71	1.13	1.79	1.42
2	73	21	0.10	0.94	2.07	1.09	1.28	1.68	1.00	1.61	1.28
3	74	21	0.10	0.94	2.07	2.40	0.82	1.45	1.01	1.60	1.17
4	75	14	0.15	0.94	2.07	2.40	0.97	2.09	1.39	2.07	1.47
5	76	15	0.14	0.94	2.07	4.47	0.92	1.94	1.30	1.88	1.16
6	77	18	0.11	0.94	2.07	4.47	0.91	1.78	1.23	1.84	1.18
7	79	14	0.15	0.94	2.07	2.57	0.71	1.52	1.01	1.50	1.09
8	82	21	0.10	1.88	1.63	2.40	0.72	1.22	0.95	1.66	1.20
9	83	18	0.11	1.88	1.63	2.40	0.70	1.26	1.02	1.73	1.25
Barda et al. <sup>26</sup>											
10	B1-1	29	0.00	0.46	2.72	2.48	1.65	3.94	1.23	0.99	1.52
11	B2-1	16	0.00	0.46	2.76	2.50	1.51	3.45	1.72	1.06	1.39
12	B3-2	27	0.00	0.46	2.72	2.56	1.48	3.23	1.18	0.93	1.29
13	B6-4	21	0.00	0.46	1.24	2.48	1.25	2.72	1.39	1.22	1.33
14	B7-5	26	0.00	0.21	2.65	2.51	1.56	4.64	1.09	0.98	1.11
15	B8-5	23	0.00	0.96	2.64	2.48	1.24	2.24	1.82	1.02	1.57
Cardenas et al. <sup>19</sup>											
16	SW-7	43	0.00	1.00	3.44	1.12	1.30	2.06	0.88	1.45	1.03
17	SW-8	42	0.00	1.00	13.45	1.26	1.36	2.02	0.97	1.28	0.96
Corley et al. <sup>27</sup>											
18	B2	54	0.00	2.40	1.54	3.35	0.76	1.31	1.04	0.92	1.04
19	B5	45	0.00	2.40	1.46	3.16	0.91	1.56	1.27	1.14	1.30
20	B6	22	0.14	2.40	1.48	3.22	1.10	1.96	1.56	1.28	1.78
21	B7	49	0.08	2.40	1.42	3.08	1.18	2.05	1.11	1.07	1.40
22	B8	42	0.09	2.40	1.32	6.65	0.94	1.38	1.13	1.00	1.31
23	B9	44	0.09	2.40	1.34	2.91	1.25	2.17	1.12	1.12	1.49
24	B10	46	0.09	2.40	1.35	2.92	0.90	1.56	0.81	0.80	1.17
25	F1	38	0.00	2.40	1.58	3.73	0.90	1.45	1.41	1.20	1.51
26	F2	46	0.08	2.40	1.44	2.92	1.13	1.96	0.91	0.91	1.28
Maeda <sup>28</sup>											
27	MAE03	58	0.03	0.55	3.83	3.83	1.46	2.82	1.02	0.96	1.09
28	MAE07	58	0.03	0.55	6.42	6.42	1.52	2.38	1.10	1.10	1.11
Okamoto <sup>29</sup>											
29	W48M6	82	0.02	0.74	4.44	4.44	1.10	1.99	0.88	0.70	1.16
30	W48M4	82	0.02	0.74	4.12	4.12	1.12	1.97	0.86	0.68	1.14
31	W72M8	82	0.02	0.74	7.24	7.24	1.33	1.89	1.20	0.95	1.41
32	W72M6	82	0.02	0.74	6.65	6.65	1.30	1.93	1.17	0.93	1.38
33	W72M8	102	0.02	0.74	7.24	7.24	1.23	1.93	1.14	0.88	1.40
34	W96M8	102	0.02	0.74	9.41	9.41	1.44	2.04	1.33	1.03	1.49
Gupta and Rangan <sup>12</sup>											
35	S-1	79	0.00	1.00	5.45	2.89	1.11	1.58	0.99	0.61	1.03
36	S-2	65	0.07	1.00	5.45	2.89	1.96	2.24	1.32	1.06	1.55
37	S-3	69	0.13	1.00	5.45	2.89	2.28	2.28	1.23	1.21	1.53
38	S-4	75	0.00	1.00	8.00	2.89	1.58	2.16	1.43	0.82	1.32
39	S-5	73	0.06	1.00	8.00	2.89	2.10	2.43	1.42	1.10	1.49



**Table 1 (cont.)—Ratio of experimental and calculated wall shear strengths**

No.	Specimen ID	$f'_c$ , MPa	$P/(f'_c A_g)$	$H_w/L_w$	$\rho_f f_{ys}$ , MPa	$\rho_w f_{yw}$ , MPa	$V_{exp}/V_n$				
							ACI 318-19 <sup>4</sup>	EC8 <sup>5</sup>	Hwang-Lee <sup>15</sup>	Kassem <sup>16</sup>	Proposed model
40	S-6	71	0.13	1.00	8.00	2.89	2.59	2.60	1.40	1.37	1.62
41	S-7	71	0.06	1.00	5.45	5.45	1.52	2.05	1.41	1.12	1.56
Kabeyasawa and Hiraishi <sup>30</sup>											
42	W-08	103	0.09	1.18	5.75	5.75	1.48	1.93	1.35	1.10	1.89
43	W-12	138	0.09	1.18	5.75	5.75	1.46	1.95	1.21	1.02	1.99
44	No. 1	65	0.13	1.18	1.58	1.58	2.25	2.19	1.11	0.91	1.48
45	No. 2	71	0.12	1.18	2.75	2.75	1.90	1.93	1.18	0.99	1.55
46	No. 3	72	0.12	1.18	4.22	4.22	1.60	1.84	1.23	1.08	1.59
47	No. 4	103	0.14	1.18	4.22	4.22	1.84	1.88	1.22	1.11	1.70
48	No. 5	77	0.11	1.76	4.22	4.22	1.41	1.50	1.07	0.94	1.55
49	No. 6	74	0.12	1.18	9.31	9.31	1.45	1.86	1.26	1.09	1.34
50	No. 7	72	0.12	1.18	7.92	7.92	1.57	2.01	1.34	1.18	1.50
51	No. 8	76	0.11	1.18	11.52	11.52	1.66	2.13	1.45	1.25	1.45
Farvashany et al. <sup>31</sup>											
52	HSCW1	104	0.04	1.25	6.74	2.51	2.20	2.36	1.56	1.00	1.62
53	HSCW2	93	0.09	1.25	6.74	2.51	2.60	2.48	1.60	1.18	1.78
54	HSCW3	86	0.09	1.25	4.01	2.51	1.96	1.85	1.19	0.91	1.38
55	HSCW4	91	0.22	1.25	4.01	2.51	2.68	1.99	1.13	1.23	1.56
56	HSCW5	84	0.09	1.25	6.74	4.01	1.93	2.07	1.42	1.18	1.66
57	HSCW6	90	0.05	1.25	6.74	4.01	1.77	1.94	1.49	1.06	1.63
58	HSCW7	102	0.08	1.25	4.01	4.01	1.85	1.94	1.39	1.08	1.67
Burgueno et al. <sup>32</sup>											
59	M05C	46	0.08	2.25	6.54	8.14	1.85	2.68	2.46	1.68	1.62
60	M05M	39	0.09	2.25	6.54	8.14	2.14	3.23	2.76	1.89	1.81
61	M10C	56	0.06	2.25	7.00	8.71	1.56	2.19	2.22	1.46	1.39
62	M10M	84	0.04	2.25	7.00	8.71	1.53	2.09	2.43	1.62	1.51
63	M15C	102	0.03	2.25	7.07	8.80	1.27	1.77	2.09	1.45	1.37
64	M15M	111	0.03	2.25	7.03	8.75	1.38	1.98	2.33	1.65	1.54
65	M20C	131	0.03	2.25	6.44	10.69	1.11	1.72	1.92	1.43	1.35
66	M20M	115	0.03	2.25	6.44	10.69	1.34	1.95	2.27	1.59	1.49
Cheng et al. <sup>33</sup>											
67	M60	39	0.00	0.94	1.39	1.39	0.92	1.76	0.69	1.24	0.93
68	M115	38	0.00	0.94	1.21	2.41	0.68	1.14	0.68	1.23	0.83
69	H60	44	0.00	0.94	3.89	3.89	0.87	1.37	1.08	1.81	1.12
70	H115	44	0.00	0.94	3.30	3.30	0.88	1.39	0.99	1.70	1.13
71	H60X	42	0.00	0.94	3.89	3.89	0.88	1.41	1.10	1.85	1.14
Teng and Chandra <sup>22</sup>											
72	J1	103	0.05	1.00	1.71	1.71	2.85	3.25	1.62	1.29	1.65
73	J2	97	0.05	1.00	4.34	1.71	3.05	3.48	1.75	1.20	1.71
74	J3	111	0.05	1.00	1.71	4.34	2.09	2.36	1.71	1.51	1.87
75	J4	94	0.05	1.00	1.71	1.71	1.97	2.35	1.44	2.06	1.19
76	J5	103	0.05	2.00	1.71	1.71	1.73	4.36	1.07	0.88	1.07
77	J6	97	0.05	2.00	4.34	1.71	2.14	5.30	1.33	0.98	1.29
78	J7	111	0.05	2.00	1.71	4.34	1.46	2.58	1.23	1.24	1.52

**Table 1 (cont.)—Ratio of experimental and calculated wall shear strengths**

No.	Specimen ID	$f'_c$ , MPa	$P/(f'_c A_g)$	$H_w/L_w$	$\rho_{f_{ys}}$ , MPa	$\rho_{f_{yh}}$ , MPa	$V_{exp}/V_n$				
							ACI 318-19 <sup>4</sup>	EC8 <sup>5</sup>	Hwang-Lee <sup>15</sup>	Kassem <sup>16</sup>	Proposed model
Baek et al. <sup>34</sup>											
79	NS2	37	0.07	2.00	5.17	4.37	1.34	2.10	1.98	3.36	1.72
80	HS2	37	0.07	2.00	3.74	4.54	1.30	2.04	1.93	3.31	1.72
81	NS2L	37	0.07	2.00	3.10	2.16	1.40	2.57	1.31	2.46	1.43
82	HS2L	37	0.07	2.00	2.80	2.27	1.45	2.63	1.41	2.64	1.54
Baek et al. <sup>35</sup>											
83	NS1M	53	0.07	1.00	5.17	4.37	1.26	1.77	1.37	2.21	1.31
84	HS1M	53	0.07	1.00	4.67	4.54	1.17	1.64	1.28	2.06	1.22
85	NS0.5M	45	0.07	0.50	4.32	4.37	1.50	2.33	1.19	2.55	1.25
86	HS0.5M	37	0.07	0.50	3.87	4.54	1.54	2.40	1.29	2.74	1.29
Baek et al. <sup>36</sup>											
87	SW1	20	0.00	2.50	0.82	1.14	0.91	1.90	1.36	2.25	1.30
88	SW2	20	0.25	2.50	0.82	1.14	1.14	2.36	0.92	1.62	1.28
89	SW3	20	0.00	2.50	0.97	1.08	0.90	1.90	1.30	2.15	1.21
90	SW4	20	0.25	2.50	0.97	1.08	1.17	2.48	0.92	1.63	1.26
91	SW5	37	0.14	2.50	0.82	1.14	1.20	2.86	0.79	1.42	1.06
92	SW6	37	0.14	2.50	0.97	1.08	1.21	2.95	0.79	1.41	1.02
Hube et al. <sup>37</sup>											
93	WSL1	29	0.00	1.00	1.21	1.21	0.85	1.31	0.77	1.29	0.87
94	WSL3	29	0.00	1.00	1.56	1.56	1.01	1.50	1.02	1.70	1.13
95	WSL4	29	0.00	1.00	0.88	0.88	1.13	1.80	0.92	1.51	1.03
96	WSL5	29	0.00	1.00	0.89	0.89	1.00	1.58	0.82	1.34	0.91
97	WSL6	29	0.00	1.00	0.62	0.62	1.12	1.86	0.84	1.34	0.92
98	WSL7	29	0.00	1.00	1.51	1.51	0.89	1.34	0.87	1.46	1.00
99	WSL8	29	0.00	1.00	1.07	1.07	0.94	1.49	0.80	1.34	0.93
100	WSL9	29	0.00	1.00	1.12	1.12	1.07	1.67	0.92	1.54	1.07
Statistical parameters											
Minimum value							0.68	1.14	0.68	0.61	0.83
Maximum value							3.05	5.30	2.76	3.36	1.99
Average value							1.41	2.13	1.29	1.40	1.35
Standard deviation							0.50	0.70	0.41	0.52	0.25
Coefficient of variation							0.35	0.33	0.32	0.37	0.19

**CONCLUSIONS**

The authors have developed an analytical method based on the strut-and-tie concept to calculate the shear strength of reinforced concrete (RC) low-rise walls. The following conclusions can be made:

1. The proposed strut-and-tie model was verified with a total of 100 RC low-rise walls (wall height-length ratio [ $H_w/L_w$ ] less than 2.5) failing in shear that were selected from available literature.<sup>12,19,22,25-37</sup> The analysis results show that the model is conservative in predicting the shear strength of RC low-rise walls with an average value of the ratio of the experimental shear strengths to calculated shear strengths  $V_{exp}/V_n$  of 1.35. While Hwang and Lee’s model<sup>15</sup> has the average value  $V_{exp}/V_n$  of 1.29, which is the closest to 1.00, it overestimates the shear strength of 22 specimens whereas the proposed model only overestimates seven specimens.

It is generally known that a strut-and-tie model serves as a lower-bound theory.<sup>14</sup>

2. As compared to building codes<sup>4,5</sup> and other strut-and-tie models,<sup>15,16</sup> the proposed strut-and-tie model has the lowest coefficient of variation (0.19) in predicting the shear strength of RC low-rise walls. This is clearly an advantage of the proposed model over other methods. In addition, the predictions of the proposed model are also quite consistent and less scattered for wide ranges of  $H_w/L_w$  and concrete compressive strengths.

**AUTHOR BIOS**

**Jimmy Chandra** is an Assistant Professor and currently Head of Structural Engineering Laboratory at Petra Christian University, Indonesia. He received his Doctor of Philosophy degree from Nanyang Technological University, Singapore. His research interests include behavior and seismic performance evaluation of reinforced concrete structures.

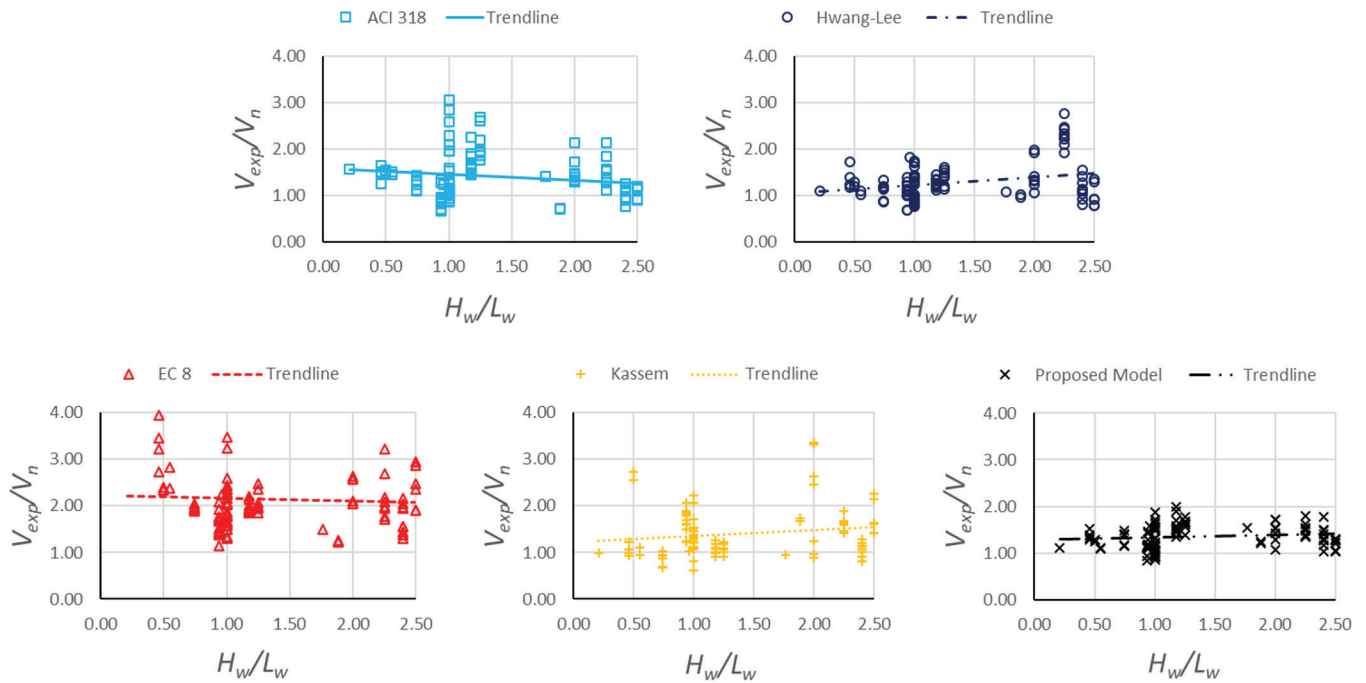


Fig. 9— $V_{exp}/V_n$  plotted against  $H_w/L_w$ .

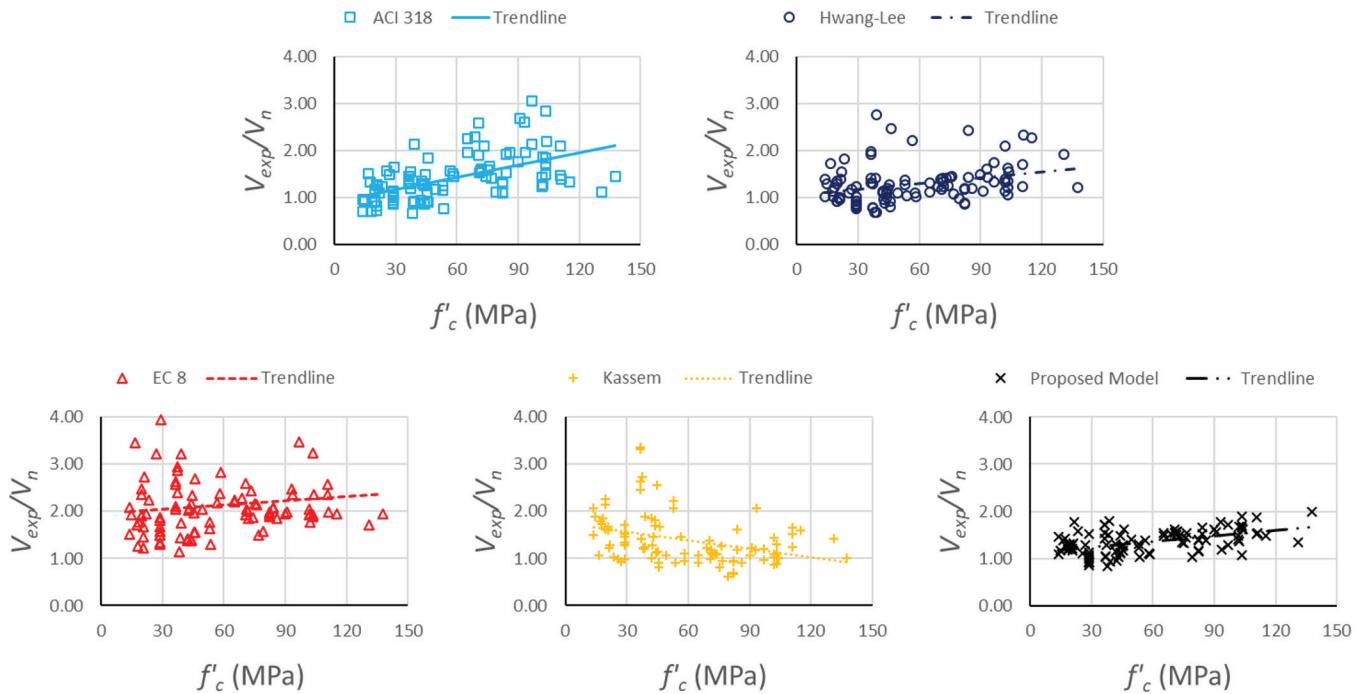


Fig. 10— $V_{exp}/V_n$  plotted against  $f'_c$ . (Note: 1 MPa = 145.04 psi).

ACI member **Susanto Teng** is an Associate Professor at Nanyang Technological University. He is a member of ACI Committee 435, Deflection of Concrete Building Structures; and Joint ACI-ASCE Committees 421, Design of Reinforced Concrete Slabs, and 445, Shear and Torsion. His research interests include behavior of structural concrete walls, shear strength of slabs, size effect in shear behavior of concrete members, computational modeling of concrete structures, and durability of marine concrete structures.

### ACKNOWLEDGMENTS

This research is part of the Competitive Research Program “Underwater Infrastructure and Underwater City of the Future” funded by the National Research Foundation (NRF) of Singapore. The authors are grateful for the funding. Support by Nanyang Technological University, Singapore,

through School of Civil and Environmental Engineering is also very much appreciated.

### NOTATION

- $A_{cv}$  = gross area of concrete section bounded by web thickness and length of section in direction of shear force considered
- $A_{civ}$  = area of concrete section of individual vertical wall segment considered
- $A_g$  = wall gross cross-sectional area
- $A_{sb}$  = total area of vertical reinforcement in one boundary element
- $A_{str}$  = area of diagonal concrete strut
- $A_{sw}$  = cross-sectional area of shear reinforcement
- $A_w$  = wall web area
- $a_s$  = depth of diagonal concrete strut
- $b_f$  = width of boundary element

$b_w$  = minimum width (thickness) of wall between tension and compression chords  
 $b_{wo}$  = width of wall web  
 $C$  = compression force in compression zone  
 $C_d$  = diagonal compression force acting on nodal zone  
 $C_{d,n}$  = nominal capacity of nodal zone  
 $c$  = depth of compression zone at bottom of wall  
 $D$  = compression force in diagonal strut  
 $D_n$  = nominal strength of diagonal concrete strut  
 $d_w$  = effective depth of wall  
 $F_h$  = tension force in horizontal tie  
 $F_v$  = tension force in vertical tie  
 $f_c'$  = concrete cylinder compressive strength  
 $f_{cd}$  = design value of concrete compressive strength  
 $f_{ck}$  = characteristic compressive cylinder strength of concrete at 28 days  
 $f_y$  = specified yield strength of reinforcement.  
 $f_{yb}$  = yield strength of vertical reinforcement in boundary element  
 $f_{yd,h}$  = design value of yield strength of horizontal web reinforcement  
 $f_{yh}$  = yield strength of horizontal shear reinforcement  
 $f_{yt}$  = yield strength of transverse reinforcement.  
 $f_{yv}$  = yield strength of vertical shear reinforcement  
 $f_{ywd}$  = design yield strength of shear reinforcement  
 $H_w$  = height of wall  
 $H'$  = distance measured from point of application of external shear force to wall base  
 $K$  = strut-and-tie index  
 $k_s$  = ratio of depth of compression zone at wall base to effective depth of wall  
 $L_w$  = wall length  
 $M_{Ed}$  = design bending moment at base of wall  
 $P$  = axial load applied at top of wall  
 $R$  = resultant force of external axial force and tension force in tension tie  
 $R_d$  = wall shear ratio resisted by diagonal mechanism  
 $R_h$  = wall shear ratio resisted by horizontal mechanism  
 $R_v$  = wall shear ratio resisted by vertical mechanism  
 $r$  = distance measured from point of application of resultant force to nearest wall edge  
 $s$  = spacing of shear (web) reinforcement  
 $T$  = tension force in tension tie  
 $t_f$  = thickness of boundary element  
 $t_w$  = thickness of wall web  
 $V$  = applied external shear force  
 $V_c$  = concrete contribution to overall shear strength  
 $V_{Ed}$  = design shear force  
 $V_{exp}$  = experimental wall shear strength  
 $V_n$  = nominal shear strength of RC wall  
 $V_{Rd}$  = shear resistance of a member with shear reinforcement  
 $V_{Rd,c}$  = design shear resistance of a member without shear reinforcement  
 $V_{Rd,max}$  = design value of maximum shear force which can be sustained by member  
 $V_{Rd,s}$  = design value of shear force which can be sustained by the yielding shear reinforcement  
 $z$  = inner lever arm, which is taken as  $0.8 L_w$  ( $L_w$  is wall length)  
 $\alpha_c$  = coefficient defining relative contribution of concrete strength to nominal wall shear strength which may be taken as 0.25 for  $H_w/L_w \leq 1.5$ , 0.17 for  $H_w/L_w \geq 2.0$ , and varies linearly between 0.25 and 0.17 for  $H_w/L_w$  between 1.5 and 2.0; where  $H_w/L_w$  is height-to-length ratio of wall  
 $\alpha_{cw}$  = coefficient taking account of state of stress in compression chord  
 $\alpha_w$  = coefficient taking account of confinement effect of web reinforcement to concrete strut strength, related to spacing of web reinforcement  
 $\lambda$  = modification factor reflecting reduced mechanical properties of lightweight concrete, all relative to normal weight concrete of same compressive strength  
 $\theta$  = angle between concrete compression strut and wall axis perpendicular to shear force (Eurocode 8)  
 $\theta$  = angle of diagonal compression strut with respect to horizontal axis (Hwang-Lee's model, Kassem's model, and proposed model)  
 $v_1$  = strength reduction factor for concrete cracked in shear  
 $\rho$  = reinforcement ratio  
 $\rho_b$  = ratio of vertical reinforcement in boundary element  
 $\rho_h$  = average horizontal web reinforcement ratio  
 $\rho_t$  = ratio of area of distributed transverse (horizontal) shear reinforcement to gross concrete area perpendicular to that reinforcement

$\rho_v$  = average vertical web reinforcement ratio  
 $\sigma_{cp}$  = mean compressive stress, measured positive, in concrete due to design axial force  
 $\omega_h$  = horizontal web reinforcement index which can be defined as  $[\rho_h f_{yh}/f_c']$   
 $\omega_v$  = vertical web reinforcement index which can be defined as  $[\rho_v f_{yv}/f_c']$   
 $\omega_w$  = coefficient taking account of confinement effect of web reinforcement to concrete strut strength, related to ratio of web reinforcement  
 $\psi$  = a non-dimensional function which can be defined as  $[0.95 - f_c'/250]$  ( $f_c'$  in MPa)  
 $\zeta$  = softening coefficient of concrete in compression

## REFERENCES

- Fintel, M., "Shearwalls – An Answer for Seismic Resistance," *Concrete International*, V. 13, No. 7, July 1991, pp. 48-53.
- Chandra, J.; Liu, Y.; and Teng, S., "Analytical Study on High Strength Concrete Shear Walls," 36th Conference on Our World in Concrete and Structures, Singapore, 2011, pp. 221-230.
- Chandra, J., and Teng, S., "Shear Strength of Normal to High Strength Concrete Walls," The 1st International Conference on Sustainable Civil Engineering Structures and Construction Materials, Yogyakarta, Indonesia, 2012, pp. 138-145.
- ACI Committee 318, "Building Code Requirements for Structural Concrete (ACI 318-19) and Commentary (ACI 318R-19)," American Concrete Institute, Farmington Hills, MI, 2019, 623 pp.
- Comite Europeen de Normalisation, "Eurocode 8: Design of Structures for Earthquake Resistance Part 1: General Rules, Seismic Actions and Rules for Buildings (EN 1998-1)," Comite Europeen de Normalisation (CEN), Brussels, Belgium, 2004.
- Ritter, W., "Die Bauweise Hennebique," *Schweizerische Bauzeitung*, V. 33, No. 7, 1899, pp. 59-61.
- Morsch, E., *Concrete-Steel Construction*, McGraw-Hill, New York, NY, 1909, 368 pp.
- Vecchio, F. J., and Collins, M. P., "Modified Compression-Field Theory for Reinforced Concrete Elements Subjected to Shear," *ACI Journal Proceedings*, V. 83, No. 2, Mar.-Apr. 1986, pp. 219-231.
- Hsu, T. T. C., "Softened Truss Model Theory for Shear and Torsion," *ACI Structural Journal*, V. 85, No. 6, Nov.-Dec. 1988, pp. 624-635.
- Hsu, T. T. C., and Mo, Y. L., "Softening of Concrete in Low-Rise Shear Walls," *ACI Journal Proceedings*, V. 82, No. 6, Nov.-Dec. 1985, pp. 883-889.
- Mau, S. T., and Hsu, T. T. C., "Shear Design and Analysis of Low-Rise Structural Walls," *JACI Journal Proceedings*, V. 83, No. 2, 1986, pp. 306-315.
- Gupta, A., and Rangan, B. V., "High-Strength Concrete (HSC) Structural Walls," *ACI Structural Journal*, V. 95, No. 2, Mar.-Apr. 1998, pp. 194-204.
- Kassem, W., and Elsheikh, A., "Estimation of Shear Strength of Structural Shear Walls," *Journal of Structural Engineering*, ASCE, V. 136, No. 10, 2010, pp. 1215-1224. doi: 10.1061/(ASCE)ST.1943-541X.0000218
- Schlaich, J.; Schafer, K.; and Jennewein, M., "Toward A Consistent Design of Structural Concrete," *PCI Journal*, V. 32, No. 3, 1987, pp. 74-150. doi: 10.15554/pci.05011987.74.150
- Hwang, S. J., and Lee, H. J., "Strength Prediction for Discontinuity Regions by Softened Strut-and-Tie Model," *Journal of Structural Engineering*, ASCE, V. 128, No. 12, 2002, pp. 1519-1526. doi: 10.1061/(ASCE)0733-9445(2002)128:12(1519)
- Kassem, W., "Shear Strength of Squat Walls: A Strut-and-Tie Model and Closed-Form Design Formula," *Engineering Structures*, V. 84, 2015, pp. 430-438. doi: 10.1016/j.engstruct.2014.11.027
- Cervenka, V., "ATENA: Software for Analysis of Concrete and Reinforced Concrete Structures," Cervenka Consulting Ltd., Prague, Czech Republic, 2012.
- Cardenas, A. E., and Magura, D. D., "Strength of High-Rise Shear Walls - Rectangular Cross Section," *Response of Multistory Concrete Structures to Lateral Forces*, SP-36, M. Fintel and J. G. MacGregor, eds., American Concrete Institute, Farmington Hills, MI, 1972, pp. 119-150.
- Cardenas, A. E.; Russell, H. G.; and Corley, W. G., "Strength of Low-Rise Structural Walls," *Reinforced Concrete Structures Subjected to Wind and Earthquake Forces*, SP-63, J. Schwaighofer, ed., American Concrete Institute, Farmington Hills, MI, 1980, pp. 221-242.
- Joint ASCE-ACI Committee 445, "Recent Approaches to Shear Design of Structural Concrete," *Journal of Structural Engineering*, ASCE, V. 124, No. 12, 1998, pp. 1375-1417. doi: 10.1061/(ASCE)0733-9445(1998)124:12(1375)

21. Park, R., and Paulay, T., *Reinforced Concrete Structures*, John Wiley & Sons, Inc., New York, 1975, 769 pp.
22. Teng, S., and Chandra, J., "Cyclic Shear Behavior of High Strength Concrete Structural Walls," *ACI Structural Journal*, V. 113, No. 6, Nov.-Dec. 2016, pp. 1335-1345. doi: 10.14359/51689158
23. Comite Europeen de Normalisation, "Eurocode 2: Design of Concrete Structures - Part 1-1: General Rules and Rules for Buildings (EN 1992-1-1)," Comite Europeen de Normalisation (CEN), Brussels, Belgium, 2004.
24. FIP Commission 3, "Practical Design of Structural Concrete," FIB - International Federation for Structural Concrete, London, UK, 1999, 113 pp.
25. Hirosawa, M., "Past Experimental Results on Reinforced Concrete Shear Walls and Analysis on Them," Building Research Institute, Ministry of Construction, Tsukuba, Japan, 1975, 279 pp.
26. Barda, F.; Hanson, J. M.; and Corley, W. G., "Shear Strength of Low-Rise Walls with Boundary Elements," *Reinforced Concrete Structures in Seismic Zones*, SP-53, N. M. Hawkins and D. Mitchell, eds., American Concrete Institute, Farmington Hills, MI, 1977, pp. 149-202.
27. Corley, W. G.; Fiorato, A. E.; and Oosterle, R. G., "Structural Walls," *Significant Developments in Engineering Practice and Research*, SP-72, M. A. Sozen, ed., American Concrete Institute, Farmington Hills, MI, 1981, pp. 77-132.
28. Maeda, Y., "Study on Load-Deflection Characteristics of Reinforced Concrete Shear Walls of High Strength Concrete - Part 1 Lateral Loading Test," Research Institute Maeda Construction Corporation, Tokyo, Japan, 1986, pp. 97-107. (in Japanese)
29. Okamoto, S., "Study on Reactor Building Structure using Ultra-High Strength Materials: Part 1. Bending Shear Test of RC Shear Wall - Outline (in Japanese)," Summaries of technical papers of annual meeting, Architectural Institute of Japan, Tokyo, Japan, 1990, pp. 1469-1470.
30. Kabeyasawa, T., and Hiraishi, H., "Tests and Analyses of High-Strength Reinforced Concrete Shear Walls in Japan," *High-Strength Concrete in Seismic Regions*, SP-176, C. W. French and M. E. Kreger, eds., American Concrete Institute, Farmington Hills, MI, 1998, pp. 281-310.
31. Farvashany, F. E.; Foster, S. J.; and Rangan, B. V., "Strength and Deformation of High-Strength Concrete Shearwalls," *ACI Structural Journal*, V. 105, No. 1, Jan.-Feb. 2008, pp. 21-29.
32. Burgueno, R.; Liu, X.; and Hines, E. M., "Web Crushing Capacity of High-Strength Concrete Structural Walls: Experimental Study," *ACI Structural Journal*, V. 111, No. 1, Jan.-Feb. 2014, pp. 37-48.
33. Cheng, M. Y.; Hung, S. C.; Lequesne, R. D.; and Lepage, A., "Earthquake-Resistant Squat Walls Reinforced with High-Strength Steel," *ACI Structural Journal*, V. 113, No. 5, Sept.-Oct. 2016, pp. 1065-1076. doi: 10.14359/51688825
34. Baek, J. W.; Park, H. G.; Shin, H. M.; and Yim, S. J., "Cyclic Loading Test for Reinforced Concrete Walls (Aspect Ratio 2.0) with Grade 550 MPa (80 ksi) Shear Reinforcing Bars," *ACI Structural Journal*, V. 114, No. 3, May-June 2017, pp. 673-686. doi: 10.14359/51689437
35. Baek, J. W.; Park, H. G.; Lee, J. H.; and Bang, C. J., "Cyclic Loading Test for Walls of Aspect Ratio 1.0 and 0.5 with Grade 550 MPa (80 ksi) Shear Reinforcing Bars," *ACI Structural Journal*, V. 114, No. 4, July-Aug. 2017, pp. 969-982. doi: 10.14359/51689680
36. Baek, J. W.; Park, H. G.; Choi, K. K.; Seo, M. S.; and Chung, L., "Minimum Shear Reinforcement of Slender Walls with Grade 500 MPa (72.5 ksi) Reinforcing Bars," *ACI Structural Journal*, V. 115, No. 3, May 2018, pp. 761-774. doi: 10.14359/51701281
37. Hube, M. A.; Maria, H. S.; Arroyo, O.; Vargas, A.; Almeida, J.; and Lopez, M., "Seismic Performance of Squat Thin Reinforced Concrete Walls for Low-rise Constructions," *Earthquake Spectra*, V. 36, No. 3, 2020, pp. 1074-1095. doi: 10.1177/8755293020906841

## APPENDIX

An example of RC wall shear strength calculation using the authors' proposed strut-and-tie model is given herein. A specimen taken from Teng and Chandra<sup>22</sup> is used—that is, Specimen J5. The procedure is given as follows (in SI units):

### Specimen J5 data:

Concrete compressive strength,  $f_c' = 103.3$  MPa  
 Wall gross cross-sectional area,  $A_g = 196,000$  mm<sup>2</sup>  
 Axial load applied at top of wall,  $P = 1012$  kN (compression)  
 Wall height,  $H_w = 2000$  mm  
 Wall length,  $L_w = 1000$  mm

Thickness of wall web,  $t_w = 100$  mm  
 Width of boundary element,  $b_f = 500$  mm  
 Thickness of boundary element,  $t_f = 120$  mm  
 Ratio of vertical reinforcement in boundary element,  $\rho_b = 0.0388$   
 Yield strength of vertical reinforcement in boundary element,  $f_{yb} = 630$  MPa  
 Ratio of vertical shear (web) reinforcement in wall,  $\rho_v = 0.0028$   
 Yield strength of vertical shear reinforcement,  $f_{yv} = 610$  MPa  
 Ratio of horizontal shear (web) reinforcement in wall,  $\rho_h = 0.0028$   
 Yield strength of horizontal shear reinforcement,  $f_{yh} = 610$  MPa  
 Experimental wall shear strength,  $V_{exp} = 595.76$  kN

### Calculation of nominal shear strength ( $V_n$ ) according to proposed strut-and-tie model:

1. Calculate  $c$  using Eq. (8) and the corresponding  $A_{str}$

$$c = L_w \left( 0.35 + 0.5 \frac{P}{f_c' A_w} + 6 \frac{A_{sb}}{A_w} \right) \left( \frac{H_w}{L_w} \right)^{-0.4} \leq d_w$$

$$c = 1000 \left( 0.35 + 0.5 \frac{1,012,000}{103.3 \times 100,000} + 6 \frac{2328}{100,000} \right) \left( \frac{2000}{1000} \right)^{-0.4}$$

$$c = 408.23 \text{ mm} \leq 880 \text{ mm (OK)}$$

Calculating  $T$  assuming yielding of reinforcement:  
 $T_1$  from vertical reinforcement in boundary element

$$T_1 = \rho_b \times b_f \times t_f \times f_{yb}$$

$$T_1 = 0.0388 \times 500 \times 120 \times 630$$

$$T_1 = 1466.64 \text{ kN}$$

$T_2$  from vertical web reinforcement that is in tension

$$T_2 = \rho_v \times (L_w - c - t_f) \times t_w \times f_{yv}$$

$$T_2 = 0.0028 \times (1000 - 408.23 - 120) \times 100 \times 610$$

$$T_2 = 80.58 \text{ kN}$$

Calculating  $r$  by taking wall edge in tension as reference point

$$r = \frac{T_1 \times \text{arm}_1 + T_2 \times \text{arm}_2 + P \times 0.5L_w}{T_1 + T_2 + P}$$

$$r = \frac{1466.64 \times 0.5 \times 120 + 80.58 \times [120 + 0.5 \times (1000 - 408.23 - 120)] + 1012 \times 500}{1466.64 + 80.58 + 1012}$$

$$r = 243.31 \text{ mm}$$

Calculate  $\theta$  using Eq. (14)

$$\theta = \tan^{-1} \left( \frac{H'}{L_w - r - 0.5c} \right)$$

$$\theta = \tan^{-1} \left( \frac{2200}{1000 - 243.31 - 0.5 \times 408.23} \right)$$

$$\theta = 75.9 \text{ degrees}$$

Then, take  $\theta = 59$  degrees

Calculating  $A_{str}$

$$A_{str} = a_s \times t_w$$

$$A_{str} = c \times \sin\theta \times t_w$$

$$A_{str} = 408.23 \times \sin 59^\circ \times 100$$

$$A_{str} = 34,992.14 \text{ mm}^2$$

2. Calculate  $\zeta$  using Eq. (10):

Calculating  $\alpha_w$  using Eq. (11)

$$\alpha_w = 1.6 \frac{s}{t_w} \leq 0.4$$

$$\alpha_w = 1.6 \frac{200}{100}$$

$$\alpha_w = 3.2$$

Then, take  $\alpha_w = 0.4$

Calculating  $\omega_w$  using Eq. (12)

$$\rho f_y = \rho_v f_{yv} \cos\theta + \rho_h f_{yh} \sin\theta$$

$$\rho f_y = 0.0028 \times 610 \times \cos 59^\circ + 0.0028 \times 610 \times \sin 59^\circ$$

$$\rho f_y = 2.34$$

$$\omega_w = 4 \frac{\rho f_y}{f_c}$$

$$\omega_w = 4 \frac{2.34}{103.3}$$

$$\omega_w = 0.09$$

$$\zeta = 0.6 (1 - f_c'/250) \times 0.80 (1 + 1.6\alpha_w\omega_w) \leq 0.85$$

$$\zeta = 0.6 (1 - 103.3/250) \times 0.80 (1 + 1.6 \times 0.4 \times 0.09)$$

$$\zeta = 0.30$$

3. Calculate  $D_n$  using Eq. (9)

$$D_n = \zeta f_c' A_{str}$$

$$D_n = 0.30 \times 103.3 \times 34,992.14$$

$$D_n = 1077.18 \text{ kN}$$

4. Calculate  $V_n$  using Eq. (15)

$$V_n = D_n \cos\theta$$

$$V_n = 1077.18 \times \cos 59^\circ$$

$$V_n = 554.79 \text{ kN}$$

Thus,  $V_{exp}/V_n = 595.76/554.79 = 1.07$ .